EPJ Web of Conferences **66**, 05006 (2014)
DOI: 10.1051/epjconf/ 20146605006

Development of narrowband lasers for spectroscopy of antiprotonic atoms

M. Hori[1,a], A. Sótér[1], and A. Dax[2]

[1] *Max-Planck-Institut für Quantenoptik, Hans-Kopfermann-Strasse 1, 85748 Garching, Germany.*
[2] *Paul Scherrer Institut, CH-5232 Villigen, Switzerland.*

Abstract. We review some lasers developed by the ASACUSA collaboration of CERN, to carry out spectroscopy of antiprotonic helium atoms. These lasers were based on the technique of continuous-wave injection seeding of pulsed lasers. The laser output covered the wavelength regions 264–1154 nm, with peak powers of ~ 1 MW and spectral resolutions of 6–40 MHz. The devices were recently used to measure the transition frequencies of antiprotonic helium atoms to a fractional precision of several parts in ~ 10^9.

1 Introduction

The ASACUSA collaboration at the Antiproton Decelerator of CERN [1] has carried out high-precision laser spectroscopy [2–6] experiments on antiprotonic helium atoms ($\overline{p}\mathrm{He}^+ \equiv \overline{p} + \mathrm{He}^{2+} + e^-$) since 1999. These are three-body Coulomb systems composed of a helium nucleus, an electron occupying the 1s- ground state, and an antiproton occupying a Rydberg state with principal and angular momentum quantum numbers of around $n \sim \ell - 1 \sim 38$. By comparing the measured frequencies of $\overline{p}\mathrm{He}^+$ with the results of three-body QED [7] calculations, the antiproton-to-electron mass ratio was recently determined [6] as $M_{\overline{p}}/m_e = 1836.1526736(23)$. This is in good agreement with the known proton-to-electron mass ratio [8]. By assuming that CPT invariance [9] is valid (i.e, $M_{\overline{p}} = M_p = 1.00727646677(10)$ u), the electron mass was determined from this experimental result on $\overline{p}\mathrm{He}^+$ as $m_e = 0.0005485799091(7)$ u [6, 8].

The precision of previous experiments on $\overline{p}\mathrm{He}^+$ was limited to around $10^{-7} - 10^{-8}$ due to the Doppler broadening effect: as in normal atoms, the thermal motions of $\overline{\mathrm{He}}^+$ in the experimental target caused the observed spectral lines to broaden. In a recent experiment [6], this Doppler broadening was partially canceled by irradiating the $\overline{p}\mathrm{He}^+$ with two counter-propagating laser beams, thereby inducing two-photon transitions of the antiproton in the atom. Sharp spectral lines were thus observed, from which the transition frequencies were determined with a higher precision than before. For this experiment, nanosecond lasers with MW-scale output energies and very low phase noise were needed to avoid rapid dephasing of the two-photon transition amplitude [10]. In this paper, we describe these lasers [11].

[a] e-mail: Masaki.Hori@mpq.mpg.de

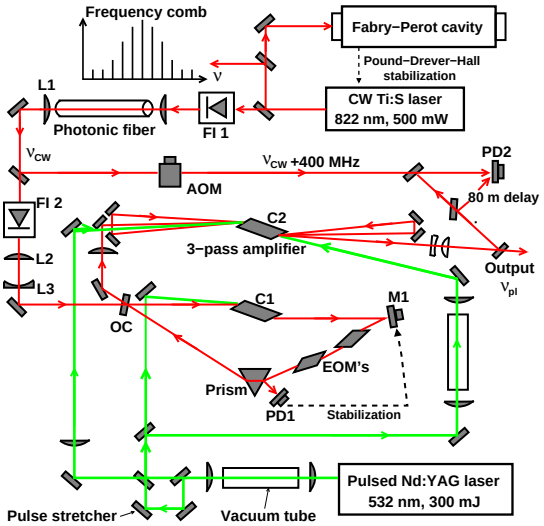

Figure 1. Layout of the Ti:sapphire laser, showing the triangular resonator used to amplify the cw seed light to a pulse energy of 8–15 mJ. An amplifying Ti:sapphire crystal is then used to increase the laser power to 50–100 mJ. A pair of intracavity electro-optic modulators correct the spurious frequency chirp. Abbreviations defined in the text. From Ref. [11].

2 Injection-seeded Ti:Sapphire lasers

A previous series of experiments on $\overline{p}\mathrm{He}^+$ was based on continuous-wave (cw) pulse-amplified dye lasers [5]. Here light from a cw laser was amplified by a factor $\sim 10^6$ in quartz cells filled with organic dye. This generated $\sim$ 10-ns-long laser pulses of peak power $\sim$ 1 MW. Similar lasers have been used for many years to measure the transition frequencies of positronium [12] and normal helium atoms [13]. It is generally difficult, however, to stabilize the optical frequency ν_{pl} of these nanosecond lasers with a high degree of precision. This is because ν_{pl} is modulated by rapid changes in the refractive index n_c of the dye gain media during the laser amplification. This so-called "chirp" effect can broaden the laser linewidth and shift its frequency by several tens MHz or more. Indeed, the linewidth of the pulsed dye laser used in Ref. [5] was typically around $\Gamma \sim 60$ MHz [5], whereas its frequency fluctuated by several tens MHz from shot to shot. This spectral resolution was nevertheless a factor $\sim$ 10 smaller than those of multi-mode lasers, which were used in the earliest spectroscopy experiments on $\overline{p}\mathrm{He}^+$ carried out by ASACUSA [3, 4, 14].

More recently, we developed ring oscillators [11] which had a circumference of $l \sim 800$ mm and included Ti:sapphire crystals as the gain media (indicated by C1 in Fig. 1). These lasers were used in the two-photon spectroscopy experiments [6] of $\overline{p}\mathrm{He}^+$. The lasers generated $\Delta t = (40 - 100)$-ns-long laser pulses of energy $E \sim$ 8–15 mJ, output wavelengths $\lambda = 726$–941 nm, and repetition rates of 0.01 – 10 Hz. This laser beam was further amplified to $E \sim$ 50–100 mJ by making three passes through another Ti:Sapphire crystal (indicated by C2). The cavity consisted of a concave mirror (M1), a flat output coupler (OC), and a prism which coarsely determined the laser wavelength. A pair of electrooptic modulators (EOM's) made of potassium dideuterium phosphate cut at Brewster's angle was placed between M1and the prism. A cw laser beam was injected into the the cavity through the mirror OC; this provided the so-called "seed" photons that were subsequently amplified in the cavity.

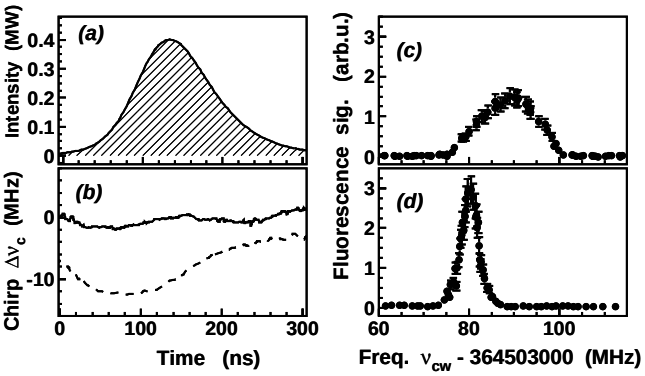

Figure 2. Time evolution of the intensity (a) and frequency chirp (b) of Ti:Sapphire laser pulses, with (solid line) and without (broken line) chirp compensation using the EOM's. The 6s-8s ($F = 4$) two-photon resonance of Cs as a function of $\nu_{\rm cw}$, without (c) and with (d) the compensation. From Ref. [11].

The cw seed beam was generated by another Ti:Sapphire laser with an output power ~ 500 mW. Its optical frequency $\nu_{\rm cw}$ was stabilized against a Fabry-Perot cavity (Fig. 1), and measured to a precision of $\sim 1\times10^{-10}$ using a femtosecond optical frequency comb [16]. The seed beam traversed two Faraday isolators (FI1 and FI2), a single-mode optical fiber, and some lenses L1–L3 before being coupled into the pulsed Ti:Sapphire cavity. The cavity length was locked to the cw seed beam to maximize the laser power circulating in the cavity.

One may naïvely expect that the optical frequencies of the seed and amplified beams would then become equal, i.e., $\nu_{\rm pl} = \nu_{\rm cw}$. As in the dye laser case, however, a spurious frequency chirp $\Delta\nu_c = \nu_{\rm pl} - \nu_{\rm cw}$ is normally induced during the amplification in laser crystals [15]. The measured time evolutions of the intensity and chirp of a typical laser pulse are shown in Figs. 2 (a)–(b). These were measured by first diverting a 2-mW part of the seed beam into an acousto-optic modulator (AOM) that shifted its frequency by +400 MHz. This cw beam was then superimposed with the pulsed beam on photodiode PD2, and the resulting heterodyne signal was recorded by a digital oscilloscope of analog bandwidth and sampling rate f=3 and 10 GHz. The optical frequency [broken lines in Fig. 2 (b)] shifted to $\Delta\nu_c(t) < -10$ MHz before returning to zero during the 100-ns-long laser pulse. Using this chirped laser, we carried out Doppler-free two-photon spectroscopy of the $F = 4$ hyperfine component in the $6s_{1/2}$-$8s_{1/2}$ two-photon transition in Cs [11]. The observed Cs line [Fig. 2 (c)] was correspondingly asymmetric and its centroid was shifted by −10 MHz relative to $\nu_{\rm cw}$. Its linewidth $\Gamma_{\rm Cs} \sim 15$ MHz was also much larger than the Fourier limit suggested by Fig. 2 (a). This causes a systematic uncertainty in our determination of the atomic transition frequency.

We next applied a sequence of stepwise high-voltage pulses of amplitude 50–150 V using a network of field-effect transistor switches [11] to the EOM's of Fig. 1, so that the resulting modulation corrected this chirp to $|\Delta\nu_c(t)| \leq 2$ MHz over most of the laser pulse [solid line in Fig. 2 (b)]. The gradients of these pulses were adjusted by tuning some load resistors and capacitors connected to the EOM's. The Cs resonance [Fig. 2 (d)] is now 3 times narrower ($\Gamma_{\rm Cs} \sim 4.5$ MHz) than in the chirp-uncorrected case. Its centroid is located at $\Delta\nu_c \sim 0$. By fitting the data with a theoretical resonance profile, the transition frequency was determined as $\nu_{6s-8s}(F = 4) = 364,503,080.3(5)$MHz [11]. This result is in good agreement with published values [17] of much higher precision.

In the experiment of Ref. [6], these lasers were used in the following way. The $\overline{p}\mathrm{He}^+$ were produced by allowing a beam of $\sim$ 100 keV antiprotons [18, 19] to come to rest in a cryogenic helium gas target. The two-photon transition was excited by simultaneously firing two counter-propagating laser beams into the target. This induced a $\overline{p}\mathrm{He}^+$ transition to a state with a short lifetime against antiproton annihilation in the helium nucleus. The resonance condition between the lasers and the atom was detected by measuring a spike in the flux of charged pions [20] emerging from these annihilations.

We have recently carried out further developmental work to improve the spectral resolutions of the dye and Ti:Sapphire lasers described here. Using these lasers, we plan to improve the experimental precision of the $\overline{p}\mathrm{He}^+$ transition frequencies. These lasers can also be used to carry out studied of the atomic cascades and state lifetimes of $\overline{p}\mathrm{He}^+$ [21–23], and laser spectroscopy of Rydberg $\overline{p}\mathrm{He}^{2+}$ ions [24], which are two-body systems composed of a helium nucleus and an antiproton. Some of the lasers described here were also used to spatially detect hydrogen gas leaking from chambers [25].

Acknowledgements

This work was supported by the European Science Foundation (EURYI) and the European Research Council (ERC-Stg).

References

[1] M. Hori and J. Walz, Progress in Particle and Nuclear Physics **72**, 206 (2013).
[2] R.S. Hayano, M. Hori, D. Horváth, E. Widmann, Rep. Prog. Phys. **70**, 1995 (2007).
[3] M. Hori *et al.*, Phys. Rev. Lett. **87**, 093401 (2001).
[4] M. Hori *et al.*, Phys. Rev. Lett. **91**, 123401 (2003).
[5] M. Hori *et al.*, Phys. Rev. Lett. **96**, 243401 (2006).
[6] M. Hori *et al.*, Nature **475**, 484 (2011).
[7] V.I. Korobov, Phys. Rev. A **77**, 042506 (2008).
[8] P.J. Mohr, B.N. Taylor, and D.B. Newell, Rev. Mod. Phys. **84**, 1527 (2012).
[9] Beringer, J. *et al.*: Review of Particle Physics. Phys. Rev. D **86**, 010001 (2012).
[10] M. Hori and V.I. Korobov, Phys. Rev. A **81**, 062508 (2010).
[11] M. Hori, A. Dax, Opt. Lett. **34**, 1273 (2009).
[12] M.S. Fee, K. Danzmann, S. Chu, Phys. Rev. A **45**, 4911 (1992).
[13] K.S.E. Eikema, W. Ubachs, W. Vassen, and W. Hogervorst, Phys. Rev. A **55**, 1866 (1997).
[14] M. Hori, R.S. Hayano, E. Widmann, H.A. Torii, Opt. Lett. **28**, 2479 (2003).
[15] V. Meyer *et al.*, Phys. Rev. Lett. **84**, 1136 (2000).
[16] Th. Udem, R. Holzwarth, T. W. Hänsch, Nature **416**, 233 (2002).
[17] P. Fendel, S.D. Bergeson, Th. Udem, T.W. Hänsch, Opt. Lett. **32**, 701 (2007).
[18] M. Hori, Nucl. Instrum. Methods Phys. Res. A **522** 420 (2004).
[19] M. Hori, Rev. Sci. Instrum. **76** 113303 (2005).
[20] M. Hori, K. Yamashita, R.S. Hayano, T. Yamazaki, Nucl. Instrum. Methods Phys. Res. A **496** 102 (2003).
[21] M. Hori *et al.*, Phys. Rev. Lett. **89**, 093401 (2002).
[22] M. Hori *et al.*, Phys. Rev. A **70**, 012504 (2004).
[23] H. Yamaguchi *et al.*, Phys. Rev. A **66**, 022504 (2002).
[24] M. Hori *et al.*, Phys. Rev. Lett. **94**, 063401 (2005).
[25] M. Hori *et al.*, Rev. Sci. Instrum. **80**, 103104 (2009).